Noname manuscript No.
(will be inserted by the editor)

The Ultraviolet-X-ray connection in AGN outflows

Elisa Costantini

Received: date / Accepted: date

Abstract In this paper I review the recent progress in understanding the physics of the gas outflowing from active galactic nuclei and its impact on the surrounding environment, using the combined information provided by multiwavelength Ultraviolet-X-ray campaigns.

Keywords X-ray Spectroscopy · UV spectroscopy · Active Galactic Nuclei · absorption lines

1 Introduction

Theoretical studies predict that the mass ejected by active galactic nuclei (AGN) has strong implications on the AGN self-sustenance (e.g. Hopkins et al. 2008) and its contribution to the environment (e.g. Ciotti et al. 2009, 2010). In particular, the outflowing gas can have an important role in host galaxy enrichment (Somerville et al. 2008, and references therein), up to larger scale environments like the intra-cluster medium (McNamara and Nulsen 2007, for a review) and eventually the intergalactic medium (e.g. Scannapieco and Oh 2004; Li et al. 2007). Metal enrichment of the environment is likely to act both at low- and high-redshift (Scannapieco et al. 2005; Martin et al. 2010). As a consequence, an impact on the cosmological quasar luminosity function is expected (e.g. Lapi et al. 2006; Hopkins et al. 2007). Ionized-gas outflows (also called warm absorbers) are detected in roughly 50% of the AGN X-ray spectra. There is a one-to- one correspondence between objects that show X-ray absorption and those that show intrinsic UV absorption, indicating that these two phenomena are related (Crenshaw et al. 1999). Multiwavelength studies of this AGN feature represent a unique tool to globally study the physics of this gas (Crenshaw et al. 2003).

E. Costantini
SRON, Netherlands Institute for Space Research, Sorbonnelaan 2, 3584CA, Utrecht, The Netherlands
E-mail: e.costantini@sron.nl

Table 1 Recent multiwavelength campaigns on bright AGN.

Object	year	Instruments	Ref.
NGC 3516	2000	LETG, STIS	1,2
NGC 3783	2000	HETG, STIS, FUSE	3,4
NGC 4051	2000	HETG, STIS	5
Mrk 509	2001	HETG, STIS	6,7
	2009	RGS, LETG, COS	8
NGC 4151	2002	HETG, STIS	9,10
NGC 7469	2002	HETG, STIS, FUSE	11
Mrk 279	2002	HETG, STIS, FUSE	12
	2003	LETG, STIS, FUSE	13,14
NGC 5548	2003	HETG, STIS	15,16
1H 0419-577	2010	RGS, COS	17

References: (1) Netzer et al. (2002), (2) Kraemer et al. (2002), (3) Kaspi et al. (2002), (4) Gabel et al. (2003), (5) Collinge et al. (2001), (6) Yaqoob et al. (2003), (7) Kraemer et al. (2003), (8) Kaastra et al. in prep., (9) Kraemer et al. (2005), (10) Kraemer et al. (2006), (11) Scott et al. (2005), (12) Scott et al. (2004), (13) Gabel et al. (2005), (14) Costantini et al. (2007), (15) Crenshaw et al. (2003), (16) Steenbrugge et al. (2005), (17) Costantini et al. in prep.

2 Early studies

Active Galactic Nuclei (AGN) have been know to host ionized gas first through their absorption and emission features in their optical spectra (Seyfert 1943). In the UV band, narrow absorption lines from low- (e.g. Mg II) and high-ionization (e.g. C IV, N V) atoms have been frequently detected by UV satellites in the 80's, (e.g. IUE; Ulrich and Boisson 1983). At the same time, many of the sources exhibiting UV absorption, showed a low-energy cut-off in the X-rays (EXOSAT; Turner and Pounds 1989). Early attempts of depicting a common origin for the UV and X-ray gas, were not successful (Ulrich 1988). The low resolution of early instruments played the major role in confusing the physical picture, as, for instance, ionized absorption could be hardly distinguished from neutral absorption. The advent of medium-resolution X-ray instruments allowed a major step forward, thanks to the detection of the O VII and O VIII (e.g. George et al. 1998). Albeit absorption features suffered from blending, e.g. O VII was blended with the iron unresolved transition array (UTA), a column density and a degree of ionization (Sect. 3.2) could be assigned to the gas absorbing the X-rays. Several studies could then put in relation the X-ray gas and the more highly ionized species (N V, C IV, Lyα) detected in the UV (e.g. Mathur et al. 1994, 1995).

3 Methods

The increase of energy resolution and sensitivity of the instruments in both UV (HST-STIS, HST-COS, FUSE) and X-ray band (*Chandra*-LETGS, *Chandra*-HETGS and XMM-*Newton*-RGS) revealed the great potential of a multiwavelength studies of this gas. This approach does not merely offer a broader-band view of the phenomenon, but allows to exploit the complementarity of the instruments to infer physical quantities. Essential ingredients of these campaigns are of course the simultaneous pointing of the AGN and an adequate exposure time, in order to maximize the signal-to-noise ratio. In Table 1 recent multiwavelength campaigns are listed, along with representative

references for the UV and X-ray analysis. Those delivered not only information on individual sources, but also provide mean properties of the gas in this class of objects. The higher spectral resolution provided in the UV band (R∼20,000) allows a detailed, velocity dependent, study of the absorption troughs of a few important ions (e.g. C IV, N V, the Lyman series, O VI). The X-rays provide a blurred (i.e. lower resolution R=400-1000) view of dozens of transitions of He- and H-like ions of C, N, O, Fe, Ne, Si and S. In the following I review in which way the information from the two bands can be combined.

3.1 Kinematics

Multiwavelength campaigns show that the UV absorber is composed by as much as four or more components with distinct outflow velocities, ranging from few tens to thousands $\mathrm{km\,s^{-1}}$(e.g. Gabel et al. 2003). The outflow velocity is measured as the displacement of the centroid of the absorption line with respect to its wavelength in the rest frame of the source, converted to velocity space. The X-ray absorbing gas usually shares some of the UV velocity components. The lower X-ray resolution however allows to assign a range of possible velocities which can be usually associated to multiple UV components with similar velocity (e.g. Kaspi et al. 2002; Steenbrugge et al. 2005). However, a higher velocity component, with no correspondence in the UV band, is sometimes detected in the X-ray band only (e.g. Collinge et al. 2001). This gas component is associated with the higher ionization ions, like O VIII, suggestive of an additional, highly ionized, gas in the system. However, no systematic correlation between outflow velocity and ionization parameter has been found in the X-rays band (Blustin et al. 2005).

3.2 Ionization parameter

An ionized gas is phenomenologically parameterized not only by its kinematic components, but also by its ionization and column density. Two similar definitions of the ionization parameter are used. The dimentionless parameter U is expressed as $U = \int_{\nu 0}^{\infty} \frac{L_\nu/h\nu}{4\pi r^2 n_{\rm H} c} d\nu$ where $L_\nu/h\nu$ is the rate of emitted photons per frequency, $n_{\rm H}$ the hydrogen number density and r the gas distance. The luminosity is integrated over the total ionizing spectrum, from ν_0, the ionization threshold of hydrogen. The other commonly used parameter is $\xi = L_{ion}/n_{\rm H} r^2$ ($\mathrm{erg\,cm\,s^{-1}}$), where L_{ion} is the integrated luminosity. Sometimes, especially in X-ray studies, ν_0 is taken as 0.1 keV (e.g. George et al. 1998). Here we will refer to the ionizing parameter as the log of ξ.

In order to find a solution for ξ, a ionization balance is needed. This expresses the balance between the recombination to and the ionization of a given ion and it is dependent on the spectral energy distribution (SED) of the source. The ionization balance is calculated using a photoionization code, such as Cloudy (Ferland et al. 1998) or XSTAR (Kallman and Bautista 2001). A grid is constructed for a range of values of ξ and $\mathrm{N_H}$ and the best fit searched through a minimizing procedure like the χ^2 or the C^2 statistical tests. In the UV band, this procedure relies on the analysis relatively few ions (Sect. 3). Despite the lower resolution, a solution for ξ and $\mathrm{N_H}$ can be easily found using X-ray data, thanks to the dozens of transitions available. In particular the presence of the iron UTA, where virtually all Fe ions are represented, helps in securing the parameter determination.

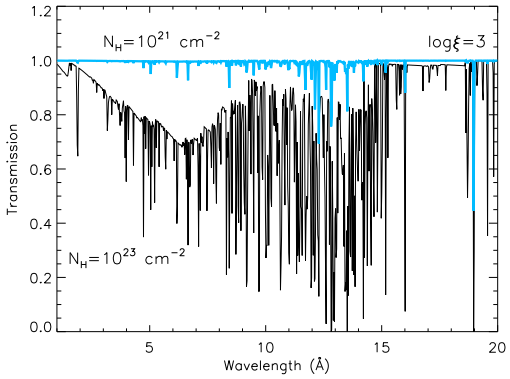

Fig. 1 Example of two highly ionized gas (logξ = 3), with differing column density. The resolution assumed is the one of the *Chandra*-HEG grating. It is evident that a high column density is necessary to clearly highlight the absorption features in an ordinary, relatively low s/n spectrum.

Higher ionization ions can be detected only in the X-ray band. Highly ionization components are highlighted mostly by H-like and He-like ions of O, Ne, Mg, Si, S and also Fe, detected at very short wavelength (λ=1.85 and 1.79 for Fe XXV and Fe XXVI, respectively). Fig. 1 shows that the opacity of such gas is modest, unless the column density becomes high ($N_{\rm H} >$ few$\times 10^{22}$ cm^{-2}). This observational bias may well be the reason why the higher ionization gas often displays a higher column density (e.g. Turner et al. 2008). There could be also low $N_{\rm H}$ gas which eluded the detection so far. It is evident however that a larger hydrogen column density is associated with the detected high ionization outflowing gas. If the UV and X-ray absorbers are co-spacial, this larger column density implies that a larger mass is associated with the X-ray absorber than with the UV absorber. Therefore the X-ray gas may play an important role in the budget of material carried away from the black hole.

3.3 Column density

In general there is a one-to-one relation between objects that show X-ray absorption and those which show UV absorption. In particular, these multiwavelength studies (Table 1) clearly pointed out that at least one UV gas component shares the same outflow velocity and ionization parameter with one X-ray component.
One major problem that confused for a while the interpretation of this phenomenon is the non-correspondence of column density between the gas detected at different frequencies. However, detailed studies revealed that the two values can be most of the times reconciled if a velocity-dependent partial covering, acting in the UV band, is allowed (e.g. Arav et al. 2002). The integrated column density of an absorption trough is $N \propto 1/\lambda f \int \tau(v) dv$, where τ is the optical depth, λ is the wavelength of the transition, f is the oscillator strength and v is the velocity. The residual intensity of a line is given by $I_1 = exp(\tau_1)$. If the line is part of the doublet (or multiplet), the optical depth ratio of two lines at ground level will be $R_{21} = f_2\lambda_2/f_1\lambda_1$. As a conse-

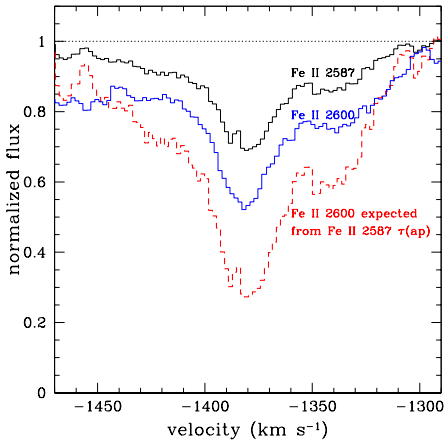

Fig. 2 Normalized residual intensity for Fe II 2587 and Fe II 2600 Å are shown. The predicted Fe II 2600 Å computed from the optical depth ratio (lower curve) fails to reproduce the observed (middle curve) data (Arav et al. 2008).

quence, the residual intensity of the other term of the doublet can be also predicted: $I_2 = exp(-R_{21}\tau_1) = I_1^{R_{21}}$. However, observations show a very different behavior, which is illustrated in Fig. 2. The observed blue part of the line multiplet is significantly shallower than predicted, implying that a covering factor $C_f(v) \simeq 1 - I_2(v)$ is at work. Accounting for $C_f(v)$, a column density compatible with the X-ray gas is obtained in most cases. The corrected column density allowed also a correct estimate of element abundances (see, e.g. de Kool et al. 2001). In at least one case, even absolute abundances could be evaluated (Arav et al. 2007). X-ray lines do not suffer dramatically from the covering factor effect in these objects, probably because the X-ray source is more compact than the UV continuum, thus the gas can more easily cover our line of sight. In one noticeable case, where the 3rd order of HETG data could be analyzed (NGC 3783, Kaspi et al. 2002), the striking similarities between the profile of Lyβ, detected in the UV, and the one of O VII, detected in the X-rays, suggests however that a covering factor could be important also for the X-ray gas (see Fig. 2 of Gabel et al. 2003). For a typical data set, higher dispersion order data, implying an enhanced energy resolution, are of poor quality. This makes impossible in practice the detection and the analysis of a velocity-dependent covering factor.

The phenomenological picture that emerges from the comparison of the absorption features in the two wave bands is that lower ionization warm absorbers are naturally detected in the UV. These are characterized by e.g. Mg II, C II. Then there is a phase which is detected in both bands. This is characterized e.g. by N V, C IV, O VI, O VII. Note that O VI is the only abundant ion which is simultaneously detected in the FUV and X-rays. Unfortunately O VI, which was successfully studied using FUSE in nearby objects (Table 1), is out of the reach of the high-resolution instruments now flying on board of HST[1]. Finally, there is a high ionization phase (log$\xi > 2$) which can be only detected in the X-rays.

[1] The O VI line enters the COS spectrograph wavelength band for redshift z> 0.1.

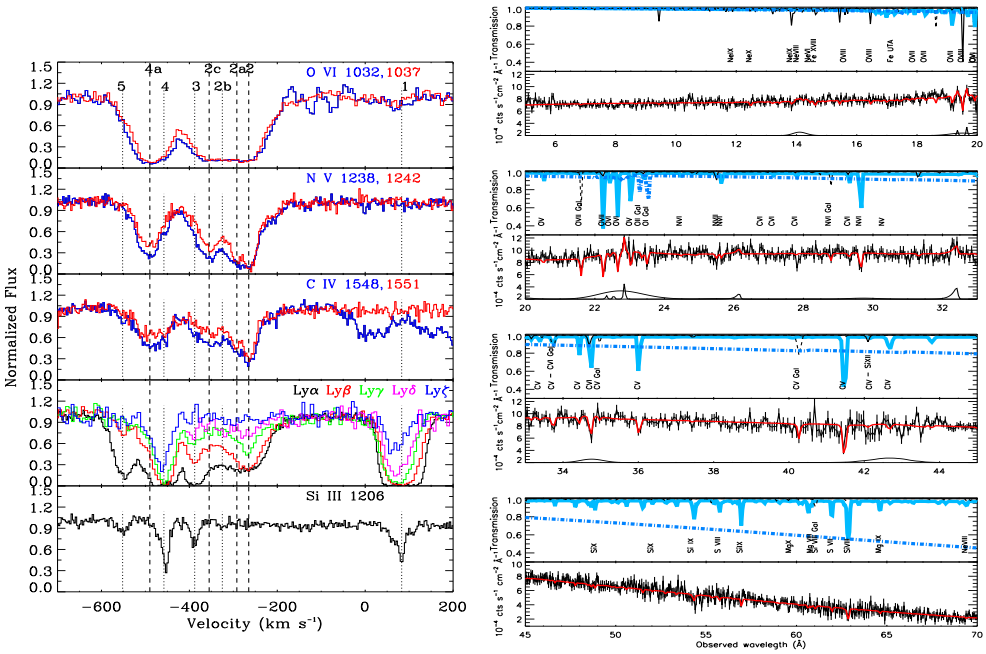

Fig. 3 (Left panel): Normalized absorption profiles from the STIS and FUSE spectra of Mrk 279. The spectra are plotted as a function of velocity with respect to the systemic redshift of the host galaxy. The dashed vertical lines identify the velocity components (Gabel et al. 2005). (Right panel): X-ray spectrum as measured by *Chandra*-LETGS along with the best fit model and the separate emission components (black lower line). In the upper panels the transmission of the gas components are shown (Costantini et al. 2007).

A typical example is given in Fig. 3 where both the UV and X-ray representative spectra of Mrk 279 are shown. The UV spectrum displays many velocity components of which only component 2 is shared with the X-rays. For that component, a full agreement of column density and ionization parameter is found in the two spectral bands (Arav et al. 2007). Lower ionization ions (e.g. Si III, Fig. 3) are represented in the UV spectrum only (Gabel et al. 2005). On the other hand, the high-ionization component, highlighted mainly by O VIII (correspondent to a log$\xi \sim 2.5$, black solid line in the upper right panels of Fig. 3) is only detected in the X-ray band (Costantini et al. 2007).

4 The origin of the UV-X-ray warm absorber

In the following I describe what are the important parameters to understand the geometry and distance of the warm absorber.

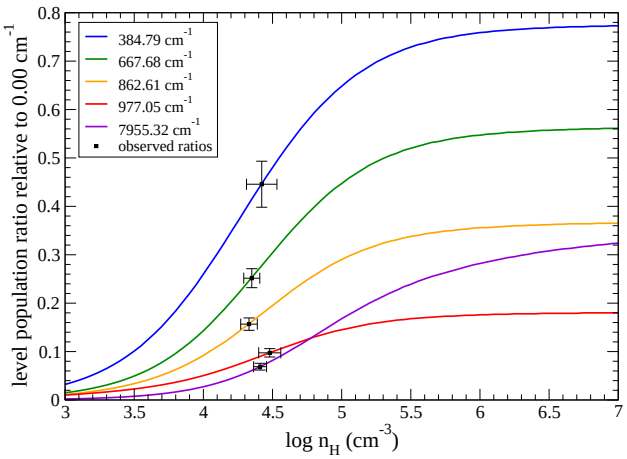

Fig. 4 Calculated level populations of excited levels of Fe II relative to the ground level as a function of the the number density. The points indicate the observed column density ratio with the ground level (in this example: QSO 2359-1241, Korista et al. 2008).

4.1 The density and distance of the gas

One of the quest in the study of the warm absorbers is the determination of the hydrogen number density of the gas. Indeed, in both energy bands there is not any straightforward method to obtain this parameter. In the UV, the most promising and accurate method is the analysis of meta-stable levels. These atomic levels are those from which the transition to the ground level is forbidden. They are populated by collisions, if the number density is above a certain threshold whose value is in turn dependent on the transition. Such experiment has been carried out e.g. using C III* and Fe II*. In Fig. 4 the practical procedure is illustrated. For each level, the theoretical relative population of the meta-stable level with respect to the ground level is plotted as a function of the number density $n_{\rm H}$. This curve is confronted with each observed relative population. It is evident that the more transitions are available, the more constrained the value of $n_{\rm H}$ will be (e.g. Gabel et al. 2005).

In the X-rays, very few Be-like ions (as C III* is) can be detected. One of them is O V*, whose main transition from the meta-stable level lies at 22.5Å. This meta-stable level is sensitive only to high densities, therefore it may be not ubiquitous in AGN spectra. A tentative detection has been reported by Kaastra et al. (2004), implying a number density $n_{\rm H} > 3 \times 10^{12}\,{\rm cm}^{-3}$.

Meta-stable levels are sensitive to only a certain range of number densities, depending on the transitions. In principle other methods, like monitoring the variability of the warm absorber in response to the central source variation, would be sensitive to any number density value, provided that the monitoring is carried out on a reasonably extended time base line. If one assumes that recombination is the only mechanism at work when the ionized gas responds to a variation in the ionizing flux, then the num-

ber density of the gas is simply inversely proportional to the recombination time (e.g. Krolik and Kriss 1995; Bottorff et al. 2000). In particular:

$\tau_{\rm rec}(X_i) = \left(\alpha_{\rm r}(X_i) n_{\rm H} \left[\frac{f(X_{i+1})}{f(X_i)} - \frac{\alpha_{\rm r}(X_{i-1})}{\alpha_{\rm r}(X_i)}\right]\right)^{-1}$,

where $\alpha_{\rm r}(X_i)$ is the recombination rate and $f(X_i)$ is the fraction of element X in ionization state i. If there is a change in column density between two epochs, the time interval between the two measurements provides a lower limit on the number density of the gas, leading to an upper limit on the distance of the gas, using the definition for the ionization parameter in Sect. 3.2. Conversely, a non-variation of the warm absorber as a function of the flux change provides a lower limit on the distance. An ideal situation is when the monitoring happens on different time scales. This allows to monitor both fast and slow flux changes and as a consequence to explore a wider range of possible densities. In practice such an ideal monitoring is difficult to perform. Brighter objects, which would provide a high s/n, securing an accurate estimate of the parameters, do not display much variability. Variations are of the order of 30% using typical exposure times (e.g. Costantini et al. 2007; Ebrero et al. 2010). The physical reason for this lack of dramatic variability is that probably they are larger systems, with larger black hole masses. Therefore, unless dedicated monitoring is performed (e.g. Mrk 509, Kaastra et al, in prep.), a comparison is done on data sets that are taken at different times, separated by months/years. Those time scales deliver only loose constraints on the number density of the gas.

Only a handful of experiments were successful in detecting significant variations of the warm absorber. For example, applying the relation for $\tau_{\rm rec}(X_i)$ and for ξ above, Krongold et al. (2005) derived an upper limit of $r < 6$ pc for the distance[2] of the gas in NGC 3783. A consistent limit of $r < 25$ pc has been derived for the same gas component from the analysis of the UV data (Gabel et al. 2005). Using the variability method on NGC 3516, a distance estimate of 0.2 pc has been obtained (Netzer et al. 2002).

Smaller black hole systems, like in the narrow line Seyfert 1 galaxies (NLS1), show instead the desired large variation in flux on time scales of few ks. An intensively studied object in this respect is NGC 4051 (e.g. Krongold et al. 2007; Steenbrugge et al. 2009). Using different instruments, variability studies point to densities which differ of a factor 20–40 for a same gas components. This mismatch underlines the challenge of this kind of analysis on complex spectra, as it relies on time-resolved spectroscopy on short time scales, which reduces the s/n considerably.

4.2 Connection between gas emission and absorption

Whether emission and absorption in both UV and X-ray band are produced from the same gas it is not clear. The main issues are that the two components do not vary on the same time scale and that the width of the lines often do not match between absorbed and emitted lines. These facts point to a different location with respect to the central source. A systematic comparison between absorption and emission is often hampered by a low s/n and by the fact that in Seyfert 1 galaxies the continuum emission is predominant, favoring the detection of absorption, rather than emission, features. Absorption lines can therefore be compared only with a handful of X-ray emission lines (typically

[2] Note that a non-variation of the warm absorber has been reported using a different data selection of the same observation (Netzer et al. 2003).

the O VII and Ne IX triplets, and O VIII) which are not always detected. In the UV, the emission spectrum is dominated by the broad emission lines whose width (2000-10,000 km s^{-1}) cannot in general be reconciled with the narrower absorption lines. Two extensively studied sources, NGC 4151 and NGC 5548 (Detmers et al. 2008) recently underwent an historically broad-band low flux. In those occasions, the UV broad lines were absent, revealing the presence of lines with smaller width (from an intermediate line region, ILR), consistently with that measured for the absorption lines. Interpreting this width as due to Keplerian broadening, a distance of 0.1 pc for both the emitting and absorbing gas has been derived in NGC 4151 (Crenshaw and Kraemer 2007). This estimate could be readily applied to the X-ray band absorbing gas, as this shared the same parameters as the UV absorbing/emitting gas. The case of NGC 5548 did not deliver a similarly simple picture, as the ILR did not have any detected absorption counterpart (Crenshaw et al. 2009). In the X-rays a direct comparison between absorption and emission has been performed e.g. on NGC 3783, for which a long XMM-*Newton* exposure allowed such a study. The similarity of the widths of emission and absorption lines and the lack of variability of the absorption features among other reasons implied a location of the gas in the narrow line region (Behar et al. 2003), in disagreement however with the estimates based on the absorption features.

5 Do outflows contribute to feedback?

Outflows are of potential crucial importance for the metal enrichment of the surrounding medium (Sect. 1). The mass for unit time carried away from the system can be expressed as:
$\dot{M}_{out} = 8\pi\mu r N_{\rm H} m_p \Omega v$,
where μ is the plasma mean molecular weight per proton ($\mu \sim 1.43$), r is the radius, $N_{\rm H}$ is the gas column density, m_p is the proton mass, Ω the global covering factor and v the outflow velocity. Collecting the values of $\dot{M}_{out}$ from classical Seyfert 1 galaxies with available distance estimates (see references in Table 1), we see that they range between 0.01–0.06 $M_\odot$ yr^{-1}. These values are often comparable with the mass accretion rate. In some outliers, $\dot{M}_{out} > 10\dot{M}_{acc}$ (e.g. Crenshaw and Kraemer 2007).
The kinetic luminosity is simply given by
$L_{kin} = 1/2\dot{M}_{out}v^2$ erg s^{-1}.
The energetics is dependent on both observable that are easy to measure (e.g. $N_{\rm H}$, v) and on the radius r, for which only in a handful of cases an estimate could be obtained. For a given radius, e.g. assuming an origin at the molecular torus distance ($\sim$0.1–5 pc in the sample presented in Table 1 of Blustin et al. 2005), then the highest column density, and most of all, fastest outflows are likely to have an impact on the surrounding medium. For the Seyfert 1 considered here, the kinetic luminosity is in general modest: $L_{kin} < 0.1\% L_{bol}$, where L_{bol} is the bolometric luminosity. Taking into account the sources where the L_{kin} value was extracted, a range of $10^{39.2-40.7}$ erg s^{-1} is obtained. Considering an AGN life-time of $\sim 4 \times 10^8$ yr (e.g. Ebrero et al. 2009), the total energy carried by the outflow is $10^{55.3-56.8}$ erg. These values, keeping in mind the associated uncertainties, may be comparable to the energy necessary to evaporate the interstellar environment out of the host galaxy ($E \sim 10^{57}$ erg, Krongold et al. 2010). An influence of the ionized flows on the intracluster medium and beyond is difficult to assess. Simulations show indeed that only an energy of about 10^{60} erg would make the outflows important at intergalactic scale (e.g. Scannapieco and Oh 2004).

6 Conclusions

Ionized outflows in Seyfert galaxies must play a role both in the self-sustenance of the active galactic nucleus and in the chemical enrichment of the environment. Multiwavelength campaigns and dedicated monitoring on interesting objects are key in extracting the most accurate parameters of the outflow. From that, also informations on the energetics of the outflow can be obtained. Although our knowledge on warm absorbers has enormously increased in the last decade, critical parameters are still extremely challenging to collect. The new HST instruments (COS, STIS) will allow easier density diagnostic studies, thanks to the high throughput. In the X-ray future, IXO will allow large monitoring campaign of warm absorbers in AGN, with minimal exposure times. The new technologies will thus allow us to quantify the impact of the outflows on the surrounding environment.

Acknowledgements I wish to thank the organizers of the "High-resolution X-ray spectroscopy: past, present, and future" conference, held in Utrecht March 15-17 2010, for inviting me to present this review. I also thank Jerry Kriss, Jacobo Ebrero and the anonymous referee for their comments on this manuscript.

References

N. Arav, K.T. Korista, M. de Kool, On the Column Density of AGN Outflows: The Case of NGC 5548. Astrophys. J. **566**, 699–704 (2002). doi:10.1086/338113

N. Arav, J.R. Gabel, K.T. Korista, J.S. Kaastra, G.A. Kriss, E. Behar, E. Costantini, C.M. Gaskell, A. Laor, C.N. Kodituwakku, D. Proga, M. Sako, J.E. Scott, K.C. Steenbrugge, Chemical Abundances in an AGN Environment: X-Ray/UV Campaign on the Markarian 279 Outflow. Astrophys. J. **658**, 829–839 (2007). doi:10.1086/511666

N. Arav, M. Moe, E. Costantini, K.T. Korista, C. Benn, S. Ellison, Measuring Column Densities in Quasar Outflows: VLT Observations of QSO 2359-1241. Astrophys. J. **681**, 954–964 (2008). doi:10.1086/588651

E. Behar, A.P. Rasmussen, A.J. Blustin, M. Sako, S.M. Kahn, J.S. Kaastra, G. Branduardi-Raymont, K.C. Steenbrugge, A Long Look at NGC 3783 with the XMM-Newton Reflection Grating Spectrometer. Astrophys. J. **598**, 232–241 (2003). doi:10.1086/378853

A.J. Blustin, M.J. Page, S.V. Fuerst, G. Branduardi-Raymont, C.E. Ashton, The nature and origin of Seyfert warm absorbers. Astron. & Astrophys. **431**, 111–125 (2005). doi:10.1051/0004-6361:20041775

M.C. Bottorff, K.T. Korista, I. Shlosman, Dynamics of Warm Absorbing Gas in Seyfert Galaxies: NGC 5548. Astrophys. J. **537**, 134–151 (2000). doi:10.1086/309006

L. Ciotti, J.P. Ostriker, D. Proga, Feedback from Central Black Holes in Elliptical Galaxies. I. Models with Either Radiative or Mechanical Feedback but not Both. Astrophys. J. **699**, 89–104 (2009). doi:10.1088/0004-637X/699/1/89

L. Ciotti, J.P. Ostriker, D. Proga, Feedback from Central Black Holes in Elliptical Galaxies. III. Models with Both Radiative and Mechanical Feedback. Astrophys. J. **717**, 708–723 (2010). doi:10.1088/0004-637X/717/2/708

M.J. Collinge, W.N. Brandt, S. Kaspi, D.M. Crenshaw, M. Elvis, S.B. Kraemer, C.S. Reynolds, R.M. Sambruna, B.J. Wills, High-Resolution X-Ray and Ultraviolet Spectroscopy of the Complex Intrinsic Absorption in NGC 4051 with Chandra and the Hubble Space Telescope. Astrophys. J. **557**, 2–17 (2001). doi:10.1086/321635

E. Costantini, J.S. Kaastra, N. Arav, G.A. Kriss, K.C. Steenbrugge, J.R. Gabel, F. Verbunt, E. Behar, C.M. Gaskell, K.T. Korista, D. Proga, J.K. Quijano, J.E. Scott, E.S. Klimek, C.H. Hedrick, X-ray/ultraviolet observing campaign of the Markarian 279 active galactic nucleus outflow: a close look at the absorbing/emitting gas with Chandra-LETGS. Astron. & Astrophys. **461**, 121–134 (2007). doi:10.1051/0004-6361:20065390

D.M. Crenshaw, S.B. Kraemer, Mass Outflow from the Nucleus of the Seyfert 1 Galaxy NGC 4151. Astrophys. J. **659**, 250–256 (2007). doi:10.1086/511970

D.M. Crenshaw, S.B. Kraemer, I.M. George, Mass Loss from the Nuclei of Active Galaxies. ARA&A **41**, 117–167 (2003). doi:10.1146/annurev.astro.41.082801.100328

D.M. Crenshaw, S.B. Kraemer, A. Boggess, S.P. Maran, R.F. Mushotzky, C. Wu, Intrinsic Absorption Lines in Seyfert 1 Galaxies. I. Ultraviolet Spectra from the Hubble Space Telescope. Astrophys. J. **516**, 750–768 (1999). doi:10.1086/307144

D.M. Crenshaw, S.B. Kraemer, J.R. Gabel, J.S. Kaastra, K.C. Steenbrugge, A.C. Brinkman, J.P. Dunn, I.M. George, D.A. Liedahl, F.B.S. Paerels, T.J. Turner, T. Yaqoob, Simultaneous Ultraviolet and X-Ray Spectroscopy of the Seyfert 1 Galaxy NGC 5548. I. Physical Conditions in the Ultraviolet Absorbers. Astrophys. J. **594**, 116–127 (2003). doi:10.1086/376792

D.M. Crenshaw, S.B. Kraemer, H.R. Schmitt, J.S. Kaastra, N. Arav, J.R. Gabel, K.T. Korista, Mass Outflow in the Seyfert 1 Galaxy NGC 5548. Astrophys. J. **698**, 281–292 (2009). doi:10.1088/0004-637X/698/1/281

M. de Kool, N. Arav, R.H. Becker, M.D. Gregg, R.L. White, S.A. Laurent-Muehleisen, T. Price, K.T. Korista, Keck HIRES Observations of the QSO FIRST J104459.6+365605: Evidence for a Large-Scale Outflow. Astrophys. J. **548**, 609–623 (2001). doi:10.1086/318996

R.G. Detmers, J.S. Kaastra, E. Costantini, I.M. McHardy, F. Verbunt, The warm absorber in NGC 5548. The lean years. Astron. & Astrophys. **488**, 67–72 (2008). doi:10.1051/0004-6361:200809862

J. Ebrero, S. Mateos, G.C. Stewart, F.J. Carrera, M.G. Watson, High-precision multi-band measurements of the angular clustering of X-ray sources. Astron. & Astrophys. **500**, 749–762 (2009). doi:10.1051/0004-6361/200911670

J. Ebrero, E. Costantini, J.S. Kaastra, R.G. Detmers, N. Arav, G.A. Kriss, K.T. Korista, K.C. Steenbrugge, XMM-Newton RGS observation of the warm absorber in Mrk 279. Astron. & Astrophys. **520**, 36 (2010). doi:10.1051/0004-6361/201014091

G.J. Ferland, K.T. Korista, D.A. Verner, J.W. Ferguson, J.B. Kingdon, E.M. Verner, CLOUDY 90: Numerical Simulation of Plasmas and Their Spectra. Pub. of the Astr. Society of the Pacific **110**, 761–778 (1998). doi:10.1086/316190

J.R. Gabel, D.M. Crenshaw, S.B. Kraemer, W.N. Brandt, I.M. George, F.W. Hamann, M.E. Kaiser, S. Kaspi, G.A. Kriss, S. Mathur, R.F. Mushotzky, K. Nandra, H. Netzer, B.M. Peterson, J.C. Shields, T.J. Turner, W. Zheng, The Ionized Gas and Nuclear Environment in NGC 3783. II. Averaged Hubble Space Telescope/STIS and Far Ultraviolet Spectroscopic Explorer Spectra. Astrophys. J. **583**, 178–191 (2003). doi:10.1086/345096

J.R. Gabel, S.B. Kraemer, D.M. Crenshaw, I.M. George, W.N. Brandt, F.W. Hamann, M.E. Kaiser, S. Kaspi, G.A. Kriss, S. Mathur, K. Nandra, H. Netzer, B.M. Peterson, J.C. Shields, T.J. Turner, W. Zheng, The Ionized Gas and Nuclear Environment in NGC 3783. V. Variability and Modeling of the Intrinsic Ultraviolet Absorption. Astrophys. J. **631**, 741–761 (2005). doi:10.1086/432682

J.R. Gabel, N. Arav, J.S. Kaastra, G.A. Kriss, E. Behar, E. Costantini, C.M. Gaskell, K.T. Korista, A. Laor, F. Paerels, D. Proga, J.K. Quijano, M. Sako, J.E. Scott, K.C. Steenbrugge, X-Ray/Ultraviolet Observing Campaign of the Markarian 279 Active Galactic Nucleus Outflow: A Global-Fitting Analysis of the Ultraviolet Absorption. Astrophys. J. **623**, 85–98 (2005). doi:10.1086/428477

I.M. George, T.J. Turner, H. Netzer, K. Nandra, R.F. Mushotzky, T. Yaqoob, ASCA Observations of Seyfert 1 Galaxies. III. The Evidence for Absorption and Emission Due to Photoionized Gas. Astrophys. J. Supp. Ser. **114**, 73 (1998). doi:10.1086/313067

P.F. Hopkins, G.T. Richards, L. Hernquist, An Observational Determination of the Bolometric Quasar Luminosity Function. Astrophys. J. **654**, 731–753 (2007). doi:10.1086/509629

P.F. Hopkins, L. Hernquist, T.J. Cox, D. Kereš, A Cosmological Framework for the Co-Evolution of Quasars, Supermassive Black Holes, and Elliptical Galaxies. I. Galaxy Mergers and Quasar Activity. Astrophys. J. Supp. Ser. **175**, 356–389 (2008). doi:10.1086/524362

J.S. Kaastra, A.J.J. Raassen, R. Mewe, N. Arav, E. Behar, E. Costantini, J.R. Gabel, G.A. Kriss, D. Proga, M. Sako, K.C. Steenbrugge, X-ray/UV campaign on the Mrk 279 outflow: Density diagnostics in Active Galactic Nuclei using O V K-shell absorption lines. Astron. & Astrophys. **428**, 57–66 (2004). doi:10.1051/0004-6361:20041434

T. Kallman, M. Bautista, Photoionization and High-Density Gas. Astrophys. J. Supp. Ser. **133**, 221–253 (2001). doi:10.1086/319184

S. Kaspi, W.N. Brandt, I.M. George, H. Netzer, D.M. Crenshaw, J.R. Gabel, F.W. Hamann, M.E. Kaiser, A. Koratkar, S.B. Kraemer, G.A. Kriss, S. Mathur, R.F. Mushotzky, K. Nandra, B.M. Peterson, J.C. Shields, T.J. Turner, W. Zheng, The Ionized Gas and Nuclear En-

vironment in NGC 3783. I. Time-averaged 900 Kilosecond Chandra Grating Spectroscopy. Astrophys. J. **574**, 643–662 (2002). doi:10.1086/341113

K.T. Korista, M.A. Bautista, N. Arav, M. Moe, E. Costantini, C. Benn, Physical Conditions in Quasar Outflows: Very Large Telescope Observations of QSO 2359-1241. Astrophys. J. **688**, 108–115 (2008). doi:10.1086/592140

S.B. Kraemer, D.M. Crenshaw, I.M. George, H. Netzer, T.J. Turner, J.R. Gabel, Variable Ultraviolet Absorption in the Seyfert 1 Galaxy NGC 3516: The Case for Associated Ultraviolet and X-Ray Absorption. Astrophys. J. **577**, 98–113 (2002). doi:10.1086/342173

S.B. Kraemer, D.M. Crenshaw, T. Yaqoob, B. McKernan, J.R. Gabel, I.M. George, T.J. Turner, J.P. Dunn, The Kinematics and Physical Conditions of the Ionized Gas in Markarian 509. II. STIS Echelle Observations. Astrophys. J. **582**, 125–132 (2003). doi:10.1086/344542

S.B. Kraemer, I.M. George, D.M. Crenshaw, J.R. Gabel, T.J. Turner, T.R. Gull, J.B. Hutchings, G.A. Kriss, R.F. Mushotzky, H. Netzer, B.M. Peterson, E. Behar, Simultaneous Ultraviolet and X-Ray Observations of Seyfert Galaxy NGC 4151. I. Physical Conditions in the X-Ray Absorbers. Astrophys. J. **633**, 693–705 (2005). doi:10.1086/466522

S.B. Kraemer, D.M. Crenshaw, J.R. Gabel, G.A. Kriss, H. Netzer, B.M. Peterson, I.M. George, T.R. Gull, J.B. Hutchings, R.F. Mushotzky, T.J. Turner, Simultaneous Ultraviolet and X-Ray Observations of the Seyfert Galaxy NGC 4151. II. Physical Conditions in the UV Absorbers. Astrophys. J. Supp. Ser. **167**, 161–176 (2006). doi:10.1086/508629

J.H. Krolik, G.A. Kriss, Observable Properties of X-Ray–heated Winds in Active Galactic Nuclei: Warm Reflectors and Warm Absorbers. Astrophys. J. **447**, 512 (1995). doi:10.1086/175896

Y. Krongold, F. Nicastro, N.S. Brickhouse, M. Elvis, S. Mathur, Opacity Variations in the Ionized Absorption in NGC 3783: A Compact Absorber. Astrophys. J. **622**, 842–846 (2005). doi:10.1086/427621

Y. Krongold, F. Nicastro, M. Elvis, N. Brickhouse, L. Binette, S. Mathur, E. Jiménez-Bailón, The Compact, Conical, Accretion-Disk Warm Absorber of the Seyfert 1 Galaxy NGC 4051 and Its Implications for IGM-Galaxy Feedback Processes. Astrophys. J. **659**, 1022–1039 (2007). doi:10.1086/512476

Y. Krongold, M. Elvis, M. Andrade-Velazquez, F. Nicastro, S. Mathur, J.N. Reeves, N.S. Brickhouse, L. Binette, E. Jimenez-Bailon, D. Grupe, Y. Liu, I.M. McHardy, T. Minezaki, Y. Yoshii, B. Wilkes, Suzaku Monitoring of the Seyfert 1 Galaxy NGC 5548: Warm Absorber Location and Its Implication for Cosmic Feedback. Astrophys. J. **710**, 360–371 (2010). doi:10.1088/0004-637X/710/1/360

A. Lapi, F. Shankar, J. Mao, G.L. Granato, L. Silva, G. De Zotti, L. Danese, Quasar Luminosity Functions from Joint Evolution of Black Holes and Host Galaxies. Astrophys. J. **650**, 42–56 (2006). doi:10.1086/507122

Y. Li, L. Hernquist, B. Robertson, T.J. Cox, P.F. Hopkins, V. Springel, L. Gao, T. Di Matteo, A.R. Zentner, A. Jenkins, N. Yoshida, Formation of z˜6 Quasars from Hierarchical Galaxy Mergers. Astrophys. J. **665**, 187–208 (2007). doi:10.1086/519297

C.L. Martin, E. Scannapieco, S.L. Ellison, J.F. Hennawi, S.G. Djorgovski, A.P. Fournier, The Size and Origin of Metal-enriched Regions in the Intergalactic Medium from Spectra of Binary Quasars. Astrophys. J. **721**, 174–192 (2010). doi:10.1088/0004-637X/721/1/174

S. Mathur, M. Elvis, B. Wilkes, Testing Unified X-Ray/Ultraviolet Absorber Models with NGC 5548. Astrophys. J. **452**, 230 (1995). doi:10.1086/176294

S. Mathur, B. Wilkes, M. Elvis, F. Fiore, The X-ray and ultraviolet absorbing outflow in 3C 351. Astrophys. J. **434**, 493–502 (1994). doi:10.1086/174750

B.R. McNamara, P.E.J. Nulsen, Heating Hot Atmospheres with Active Galactic Nuclei. ARA&A **45**, 117–175 (2007). doi:10.1146/annurev.astro.45.051806.110625

H. Netzer, D. Chelouche, I.M. George, T.J. Turner, D.M. Crenshaw, S.B. Kraemer, K. Nandra, The Density and Location of the X-Ray-absorbing Gas in NGC 3516. Astrophys. J. **571**, 256–264 (2002). doi:10.1086/338967

H. Netzer, S. Kaspi, E. Behar, W.N. Brandt, D. Chelouche, I.M. George, D.M. Crenshaw, J.R. Gabel, F.W. Hamann, S.B. Kraemer, G.A. Kriss, K. Nandra, B.M. Peterson, J.C. Shields, T.J. Turner, The Ionized Gas and Nuclear Environment in NGC 3783. IV. Variability and Modeling of the 900 Kilosecond Chandra Spectrum. Astrophys. J. **599**, 933–948 (2003). doi:10.1086/379508

E. Scannapieco, S.P. Oh, Quasar Feedback: The Missing Link in Structure Formation. Astrophys. J. **608**, 62–79 (2004). doi:10.1086/386542

E. Scannapieco, J. Silk, R. Bouwens, AGN Feedback Causes Downsizing. Astrophys. J. Letters

635, 13–16 (2005). doi:10.1086/499271

J.E. Scott, G.A. Kriss, J.C. Lee, N. Arav, P. Ogle, K. Roraback, K. Weaver, T. Alexander, M. Brotherton, R.F. Green, J. Hutchings, M.E. Kaiser, H. Marshall, W. Oegerle, W. Zheng, Intrinsic Absorption in the Spectrum of Markarian 279: Simultaneous Chandra, FUSE, and STIS Observations. Astrophys. J. Supp. Ser. **152**, 1–27 (2004). doi:10.1086/382748

J.E. Scott, G.A. Kriss, J.C. Lee, J.K. Quijano, M. Brotherton, C.R. Canizares, R.F. Green, J. Hutchings, M.E. Kaiser, H. Marshall, W. Oegerle, P. Ogle, W. Zheng, Intrinsic Absorption in the Spectrum of NGC 7469: Simultaneous Chandra, FUSE, and STIS Observations. Astrophys. J. **634**, 193–209 (2005). doi:10.1086/496911

C.K. Seyfert, Nuclear Emission in Spiral Nebulae. Astrophys. J. **97**, 28 (1943). doi:10.1086/144488

R.S. Somerville, P.F. Hopkins, T.J. Cox, B.E. Robertson, L. Hernquist, A semi-analytic model for the co-evolution of galaxies, black holes and active galactic nuclei. Monthly Notices of the Royal Astronomical Society **391**, 481–506 (2008). doi:10.1111/j.1365-2966.2008.13805.x

K.C. Steenbrugge, J.S. Kaastra, D.M. Crenshaw, S.B. Kraemer, N. Arav, I.M. George, D.A. Liedahl, R.L.J. van der Meer, F.B.S. Paerels, T.J. Turner, T. Yaqoob, Simultaneous X-ray and UV spectroscopy of the Seyfert galaxy NGC 5548. II. Physical conditions in the X-ray absorber. Astron. & Astrophys. **434**, 569–584 (2005). doi:10.1051/0004-6361:20047138

K.C. Steenbrugge, M. Fenovčík, J.S. Kaastra, E. Costantini, F. Verbunt, High-resolution X-ray spectroscopy of the low and high states of the Seyfert 1 galaxy NGC 4051 with Chandra LETGS. Astron. & Astrophys. **496**, 107–119 (2009). doi:10.1051/0004-6361/200810416

T.J. Turner, K.A. Pounds, The EXOSAT spectral survey of AGN. Monthly Notices of the Royal Astronomical Society **240**, 833–880 (1989)

T.J. Turner, J.N. Reeves, S.B. Kraemer, L. Miller, Tracing a disk wind in NGC 3516. Astron. & Astrophys. **483**, 161–169 (2008). doi:10.1051/0004-6361:20078808

M. Ulrich, Far-ultraviolet absorption lines in active galaxies. Monthly Notices of the Royal Astronomical Society **230**, 121–130 (1988)

M.H. Ulrich, C. Boisson, The ultraviolet spectrum of the Seyfert galaxies NGC 3516 and NGC 5548. Astrophys. J. **267**, 515–527 (1983). doi:10.1086/160888

T. Yaqoob, B. McKernan, S.B. Kraemer, D.M. Crenshaw, J.R. Gabel, I.M. George, T.J. Turner, The Kinematics and Physical Conditions of the Ionized Gas in Markarian 509. I. Chandra High Energy Grating Spectroscopy. Astrophys. J. **582**, 105–124 (2003). doi:10.1086/344541